2019_11_06

Fall 2019, Ceramics (5000/4000 level course)

Rishi Raj (303.492.1029); rishi.raj@colorado.edu

•The course is divided into the following topics. The topics concentrate mostly (but not exclusively) on zirconia as the ceramic material of interest.

I. Elastic deformation and fracture
II. Sintering and Superplastic Forming
III. Electrochemical applications: fuel cells, batteries, gas sensors, gas separation and catalysis

•For each topic you will have practice homework questions which you may work on by yourself or with friends. These will not be graded, but I can discuss the answers in class (no written solutions).

•At the end of each topic you will have an in-depth take home HW (essentially like an exam). You will have ten days to submit your answers (e.g. Monday to Friday of the following week).

•Each such take home HW will carry 25% of the grade.

•The remaining 25% will be based upon a 15-20 min presentation on a topic of your choice (towards the end of the semester). I will provide feedback on your presentations starting in early November so please submit your preliminary ppt file by then.

HW-TakeHomeExam-2 Elasticity and Transformation Toughening

Please submit your solutions on Monday November 18, 2019

This take home carries 25% of the grade. All questions carry equal weight. This Exam will cover material taught until, approximately, Wed. Nov 13.

1. In one page draw and/or write *three* iconic sketches and/or equations which you feel embody the subject matter we discussed in class during this second phase of the course with a focus on processing. Explain each "object" in two lines of text.

2. Consider the reaction for the oxidation of titanium

$$Ti(c)+O_2(g)=TiO_2(c) \qquad (1)$$

where, "c" stands for the pure crystal phases of titanium and its oxide, and "g" for pure gas phase of oxygen.

(a) Show that the above equation in equilibrium is expressed by

$$\Delta G^{TiO_2}_{JANAF} + RT\ell n\frac{a_{TiO_2}}{a_{Ti}a_{p_{O_2}}} = 0 \qquad (2)$$

Where "a" stands for the activity of each of the three species. ΔG_{JANAF} is the free energy of formation of TiO_2 from elements in their standard states (as given by their activities being equal to unity); its values as a function of temperature are listed in JANAF TABLES. If titanium oxide and titanium are chemically pure their activities are equal to unity. The activity for oxygen is equal to its partial pressure. (Hint: use the equation $\mu_{Ti} + \mu_{O_2} = \mu_{TiO_2}$ for equilibrium and $\mu = \mu^o + RT\ell n(a)$ for each of the species)

2.(a) Show how the above Eq. (2) is used to construct the Ellingham diagram for the reaction in Eq. (1) so that it can be read immediately to discern the equilibrium value of p_{O_2} at any temperature. In your response draw sketches with the appropriate axes to explain your thoughts. Explain explicitly how the sketches can be read for the equilibrium value of p_{O_2}.

(b) Using the attached Ellingham diagram obtain the values for $\Delta G^{TiO_2}_{JANAF}$ in the form of a numerical equation with approximately linear dependence on T(K).

3. Solid State Diffusion is described by the following equation

$$J_A = \frac{C_A D_A}{RT}\frac{d\mu_A}{dx} \qquad (3)$$

(a) Define each of the above parameters, and give their units. Show that Eq. .(3) has balanced units.

(b) You are given that the chemical potential of A may be written as

$$\mu_A = \mu^o_A + RT\ell n\mathrm{X}_A \qquad (4)$$

where μ_A^o is the potential in the standard state and X_A is the *molar concentration* of A in the host material. Show that Eq. (4) when combined with Eq. (3) reduces to the Fick's First Law

$$J_A = D_A \frac{dC_A}{dx} \qquad (5)$$

Make sure you pay attention to the units.

4. The parabolic oxidation equation (for example for the time-dependent growth of the silica over-layer, *h*, during oxidation of silicon, is as follows

$$h(t)^2 = k_p t \qquad (6)$$

(a) Obtain the expression for k_p in terms of the parameters contained in Eqns (3) and (5).

(b) Use the data given in the attached manuscript obtain a value for the thickness of the overgrowth on silicon over a period of 10 days at 1000 °C.

5. The sintering process is the densification of a porous body assembled from particles of the ceramic material. Show how mass transport by solid state diffusion can link diffusion on the atomic scale to diffusion flux on the particle size scale, and finally to the physical scale of the workpiece being sintered.

6. (a) Write half a page on what is surface tension and what is surface energy, and what may be the difference between them.
(b) In the following half page describe an experiment to measure surface tension and/or surface energy.

7. (a) Show that the curved surface of a material (it may be glass, or a crystalline ceramic) produces an inward "pull" or the surface, given by a pseudo hydrostatic tension, but written formally as t_n or normal traction, with units of force acting per unit area of surface, by

$$t_n = \frac{2\gamma_S}{r} \qquad (7)$$

where t_n has a positive value when the force is pulling outwards from the "concave" surface with a radius of curvature equal to "r". Derive Eq. (7) using the principle of virtual work.

Calculate the value for t_n in MPa for a pore of radius 1 μm. Assume that $\gamma_S = 1\,\mathrm{Jm}^{-2}$.

(b) A spherical water droplet experiences a pressure within it which is also given by Eq. (7). Show that this pressure increase linearly with the surface to volume ratio of the droplet. Calculate this pressure for a droplet size (diameter) of 10 μm, 1 μm, and 10 nm.

8. Consider a cylindrical pore formed at the junction of three crystals (also in the shape of cylinders) meeting at a triple junction, that is oriented 6o° with respect to one another.

Assume that the shape of the pore is in equilibrium so that

$$\gamma_B = 2\gamma_S \cos\theta \qquad (8)$$

where γ_B is the energy (per unit area) for the grain boundary, and θ is the dihedral angle.

(a) Show in a sketch how and why Eq. (8) is valid.

(b) Explain why the cylindrical pore will grow if $\theta < 60^o$, and shrink if $\theta < 60^o$.

9. Consider the sintering of a bi-crystal containing cylindrical pores, parallel to one another, and spaced a distance λ apart in the interface plane, aligned normal to the plane of the paper. Assume the dihedral angle $\theta = 45^o$, and the initial radius of the pores to be r_o. Develop the equation for the time required for the pores to sinter to make a pore free interface based upon Eq. (3), and the relation between the chemical potential of the species (in this instance the material itself) on the surface of the pores and the normal traction of the surface, t_n, to be given by

$$\Delta\mu_A = -t_n\Omega \qquad (9)$$

when the dominant mechanism of mass transport is by boundary diffusion, denoted by D_{gb}. In Eq. (9) Ω is the volume per atom (or molecule) of the species. In this instance the gas constant R (units of J $mol^{-1}K^{-1}$) is replaced by the Boltzmann's constant, $k_B = \frac{R}{N_{AV}}$ where N_{AV} is the Avogadro's number. Pay attention to units throughout your derivation.

10. Draw an Arrhenius graph of sintering time versus (1/T(K)) for sintering of aluminum oxide (alpha phase), with an initial particle size of 100nm. Assume grain boundary diffusion to be the dominant mechanism. The diffusion data is found at http://engineering.dartmouth.edu/defmech/, Chapter 14. Note that the slower of the two (the metal ion and the oxygen ion) will control the overall rate of diffusion. Use a temperature range of 1200 °C to 1600 °C in your Arrhenius plot. In this plot the horizontal scale can be 1000/T(K), with a parallel scale on the top of the grapn in °C so that the temperature can be read quickly. Also the vertical scale should be log to the base of 10, with tick marks showing 2, 4, 8 etc.

11. By simple arguments show that the effective diffusion coefficient for sintering is given by

$$D_{eff} = D_V + \alpha \frac{\delta_{gb} D_{gb}}{d} \qquad (10)$$

where D_V is the diffusion coefficient through the crystal matrix, δ_{gb} is the effective width of the grain boundary, d is the particle size, and α is a geometrical factor of order unity (it can be formally shown to be equal to "pi").

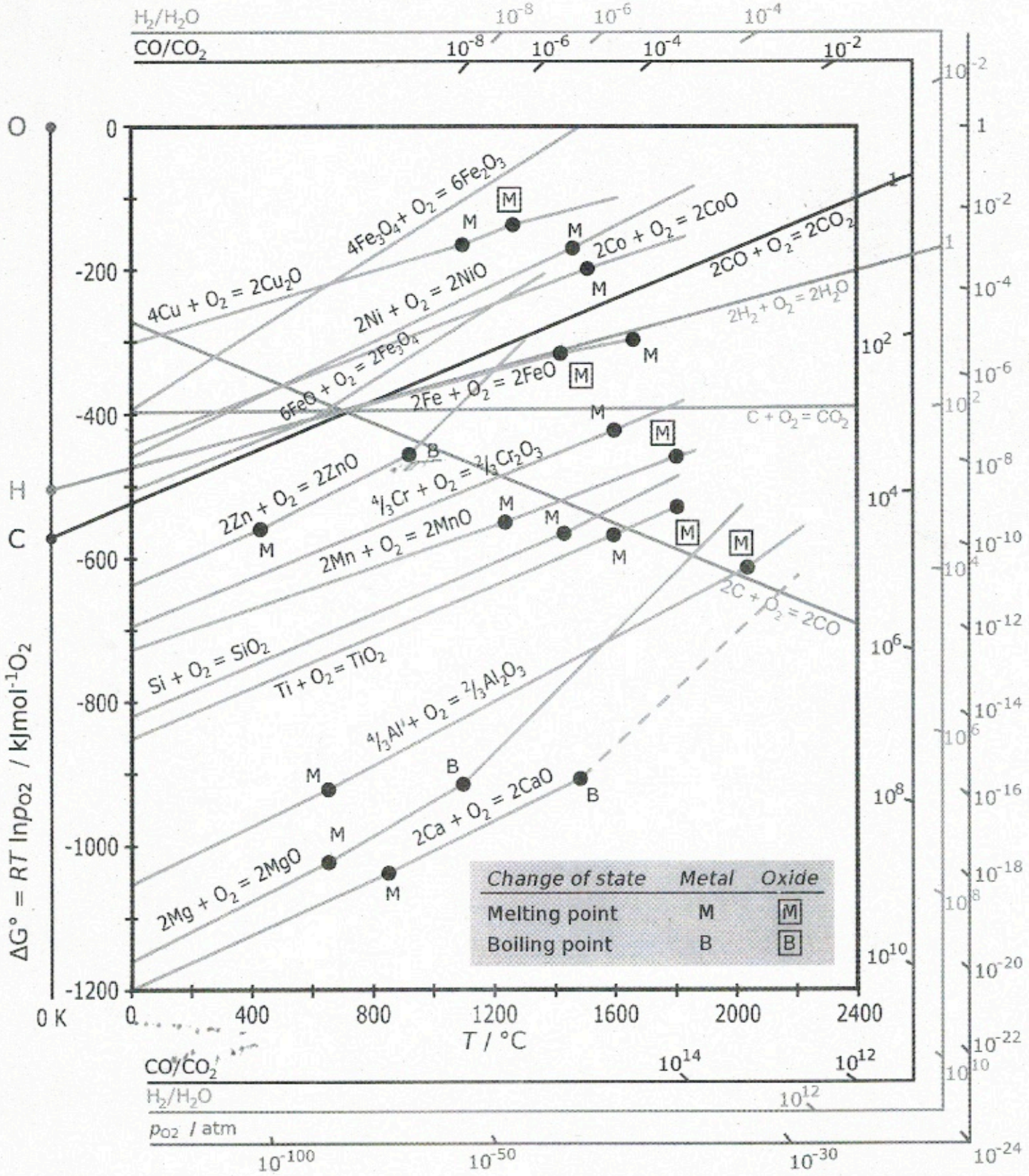
H2/H2O
CO/CO2
O
H
C
0 K
ΔG° = RT lnpO2 / kJmol-1O2
T / °C
0
-200
-400
-600
-800
-1000
-1200
400
800
1200
1600
2000
2400
4Fe3O4 + O2 = 6Fe2O3
4Cu + O2 = 2Cu2O
2Ni + O2 = 2NiO
2Co + O2 = 2CoO
2CO + O2 = 2CO2
2H2 + O2 = 2H2O
6FeO + O2 = 2Fe3O4
2Fe + O2 = 2FeO
C + O2 = CO2
2Zn + O2 = 2ZnO
4/3Cr + O2 = 2/3Cr2O3
2Mn + O2 = 2MnO
2C + O2 = 2CO
Si + O2 = SiO2
Ti + O2 = TiO2
4/3Al + O2 = 2/3Al2O3
2Mg + O2 = 2MgO
2Ca + O2 = 2CaO
M
B
Change of state
Metal
Oxide
Melting point
M
M
Boiling point
B
B
pO2 / atm

octahedral sites. The unoccupied octahedral sites are ordered within each close-packed layer, and alternate between layers, repeating every third layer. The hexagonal unit cell contains six oxygen layers.

These oxides are generally harder and more refractory than the rock-salt structured oxides, retaining their strength to higher temperatures. Alumina is used as a structural ceramic, as well as an abrasive and a coating for cutting tools. Chromium sesquioxide is perhaps most important as a surface layer on stainless steels and nickel-based alloys.

Maps for the three oxides are shown in Figs. 14.1 to 14.8. The parameters used to construct them are listed in Table 14.1.

TABLE 14.1 Oxides with tbe a-alumina structure

Material	Al_2O_3		Cr_2O_3		Fe_2O_3	
Crystallographic and thermal data						
Atomic volume, $\Omega(m^3)$	4.25×10^{-29}		4.81×10^{-29}	(h)	5.03×10^{-29}	
Burger's vector, b (m)	4.76×10^{-10}		4.96×10^{-10}	(h)	5.03×10^{-29}	(o)
Melting temperature, T_M (K)	2320		2710		1840	
Modulus						
Shear modulus at 300 K, $\mu_0(MN/m^2)$	1.55×10^5	(a)	1.30×10^5	(i)	8.82×10^4	(p)
Temperature dependence of modulus, $\frac{T_M}{\mu_0}\frac{d\mu}{dT}$	–0.35	(a)	–0.33	(j)	-0.2	(q)
Lattice diffusion: oxygen ion						
Pre-exponential, D_{0v} (m^2/s)	0.19	(b)	1.59×10^{-3}	(k)	2.04×10^{-4}	(r)
Activation energy, Q_v (kJ/mole)	636	(b)	423	(k)	326	(r)
Lattice diffusion: metal ion						
Pre-exponential, $\delta D_{0v}(m^2/s)$	2.8×10^{-3}	(c)	—		40	(s)
Activation energy, Q_v (kJ/mole)	477	(c)	—		469	(s)
Boundary diffusion: oxygen ion						
Pre-exponential, δD_{0b} (m^3/s)	10^{-8}	(d)	10^{-15}	(l)	4×10^{-13}	(t)
Activation energy, Q_b (kJ/mole)	380	(d)	240	(l)	210	(u)
Boundary diffusion: metal ion						
Pre-exponential, δD_{0b} (m^3/s)	8.6×10^{-10}	(e)	—		—	
Activation energy, Q_b (kJ/mole)	419	(e)	—		—	

journal

J. Am. Ceram. Soc., 1–9 (2013)
DOI: 10.1111/jace.12464

Chemical Potential-Based Analysis for the Oxidation Kinetics of Si and SiC Single Crystals

Rishi Raj†

Department of Mechanical Engineering, University of Colorado, Boulder 80309, Colorado

A one-dimensional diffusion problem with prescribed boundary conditions for the oxygen potential at the oxygen(gas)–silica and at the silica–substrate interfaces is employed to obtain the parabolic rate constant for oxidation of Si crystals. The results, using the data for diffusion and solubility of molecular oxygen in silica agree reasonably well with the oxidation kinetics results for Si from Deal and Grove (1965). The measurements for SiC crystals (Costello and Tressler, 1985) lie below these results for Si, even though in both instances, diffusion through the silica overlayer is expected to have been rate controlling. This difference is explained in terms of the lower Si activity at the SiC–SiO_2 interface than at the Si–SiO_2 interface. The implication of the interface structure is discussed in an attempt to explain the higher activation energy for oxidation of the Si-face (0001), than the C-face $(000\bar{1})$ of SiC crystals.

I. Introduction

The results from the oxidation of silicon crystals studied by Deal and Grove (D&G[1]), from 700°C to 1200°C in dry oxygen ($p_{O_2} = 1$), are reproduced in Fig. 1. They show that at high temperatures, the oxidation behavior is predominantly parabolic, but exhibits a trend toward interface control in early oxidation. For example, note that the transition from interface control to diffusion control occurs at a scale thickness of approximately ~30 nm at 700°C. At higher temperatures, this transition occurs earlier, when the overgrowths are even thinner. The implication is that studies of the early stages of oxidation are likely to have emphasized interface-controlled oxidation behavior. Interface-controlled oxidation, which dominates at lower temperatures in thin films, is of interest to the microelectronics community.[2,3] However, in structural ceramics, where the temperatures are high and the overgrowths are thick, the diffusion-controlled, parabolic regime is more important.

The parabolic equation for oxidation is derived by assuming that the growth rate is inversely proportional to the thickness of the oxide scale. It has usually been explained by invoking Fick's law whereby the driving force for the diffusion of oxygen is proportional to the difference in the concentration of oxygen at the surface and at the substrate interface divided by the thickness of the scale. In this approach, the surface concentration is set to be proportional to p_{O_2} in the environment, and to a negligible value at the interface, for example see Ref. [4].

The concentration profiles of molecular oxygen have been charted by Cawley *et al.*[5] with ^{18}O isotope. They found the concentration was flat, and low, in the middle of the scale, but higher both near the surface and at the buried interface. These findings have been confirmed in later studies, e.g.,[6] These measurements are inconsistent with models that rely on linear concentration gradients through the oxide scales. Furthermore, the assumption of near zero concentration at the interface needs to be reconciled with the fact that a significant concentration of oxygen molecules must be present at the interface for silicon to convert to silica at the measured rates.

The analysis of oxidation must also ask the question whether the dominant diffusing species is atomic, ionic, or molecular oxygen. Two main results point toward oxygen molecules as being the dominant mechanism: (i) the strictly linear dependence of the parabolic rate on the partial pressure of oxygen ranging from 0.1 to 1.0, at temperatures from 1000°C to 1200°C as reported by D&G in their figure 8, and (ii) state-of-the-art DFT calculations[7] show that 3.4 eV is needed to disassociate an interstitial O_2 molecule into two interstitial oxygen atoms (the energy to break the network Si–O bond to form ionic oxygen is even greater), a value much larger than the activation energy for the growth of the oxide scale measured by D&G, which was equal to 119 kJ/mol or 1.23 eV. The activation energy for diffusion of O_2 through seven-membered rings in the silica network calculated by Stoneham *et al.*[7] is in the range 1.2–1.3 eV (115–123 kJ/mol), consistent with the activation energies for the growth of the silica overlayer. The relative values for O_2 migration through five- and six-membered rings were significantly greater than the measured activation energies.[7]

Oxidation of silicon-carbide can be expected to be similar to that of silicon as in both instances, the silica overgrowth provides the passivation protection. Results from Costello and Tressler[8,9] for single crystals of SiC, replotted in Fig. 2, conclusively show, similar to silicon, that the rate is parabolic in the range 1200°C–1500°C. However, when the parabolic rate constants for Si and SiC are compared, as shown in Fig. 3, two notable features emerge: (i) the rate constant is significantly slower for SiC, and (ii) the Si- and the C-face of (0001) orientation of SiC crystals oxidize differently: while the carbon face has a similar activation energy as D&G, the silicon face exhibits a significantly higher activation energy, and lies below the C-face data. This behavior has been a topic of considerable interest in the literature.[10] We seek to present a hypothesis for this behavior.

The above observations and measurements are coalesced into a unified model by employing the chemical potential of O_2, written as μ_{O_2}, to analyze the oxidation kinetics of Si and SiC. μ_{O_2} is exactly defined at the surface (by the oxygen partial pressure in the environment), and at the interface (by the equilibrium between Si and SiO_2). It then becomes a matter of solving a one-dimensional boundary value problem, which is shown to give agreement with D&G. In the case of SiC, the interfacial μ_{O_2} depends on the activity of silicon at the interface. We attribute the divergence between the Si-face and C-face data to the difference in the activity of silicon at these interfaces.

J. Smialek—contributing editor

Manuscript No. 32302. Received November 8, 2012; approved May 20, 2013.
†Author to whom correspondence should be addressed. e-mail: rishi.raj@colorado.edu

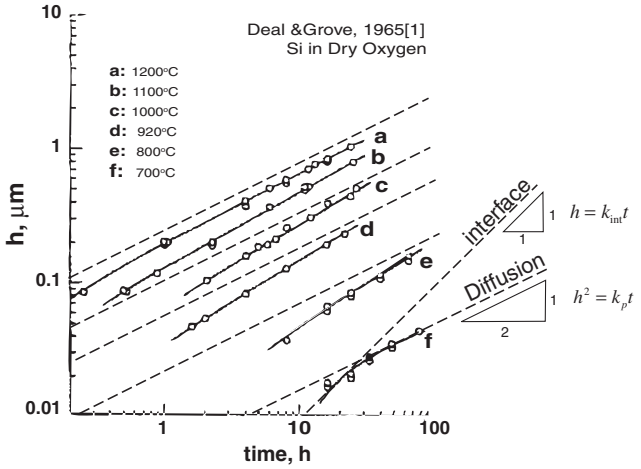

Fig. 1. A logarithmic plot of the thickness of the overgrowth versus time. The ideal slopes for interface and diffusion control are shown in dashed lines.

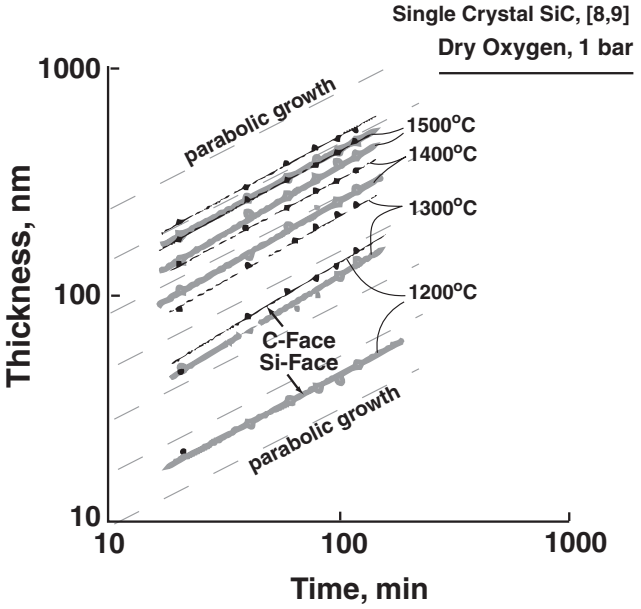

Fig. 2. Logarithmic plots of thickness versus time data for the Si- and the C-face orientations of SiC single crystals. The slopes of the dashed lines represent ideal parabolic oxidation.

II. Oxidation of Silicon Crystals

(1) A Model Based Upon Chemical Potentials of Oxygen

The oxidation of silicon when formulated in terms of the chemical potential gradients of μ_{O_2} becomes a simple boundary value problem where the diffusion flux is given by the equation:

$$J_{O_2} = -\frac{D_{O_2} n_{O_2}}{V_{SiO_2} RT} \frac{d\mu_{O_2}}{dz} \tag{1}$$

Here, D_{O_2} is the chemical diffusion coefficient of O_2, n_{O_2} is the molar concentration of oxygen in silica, and V_{SiO_2} is the molar volume of silica. The temperature, T, is in Kelvin and R is the gas constant [8.31 J·(mol·K)$^{-1}$]. Note that J_{O_2} has the following units: moles of oxygen flowing across a unit cross section per unit time (m^{-2}s^{-1}).

The application of Eq. (1) requires a boundary value problem where the chemical potentials are prescribed at the interfaces where the oxygen molecules are absorbed or consumed. Within the material, the problem can then be solved

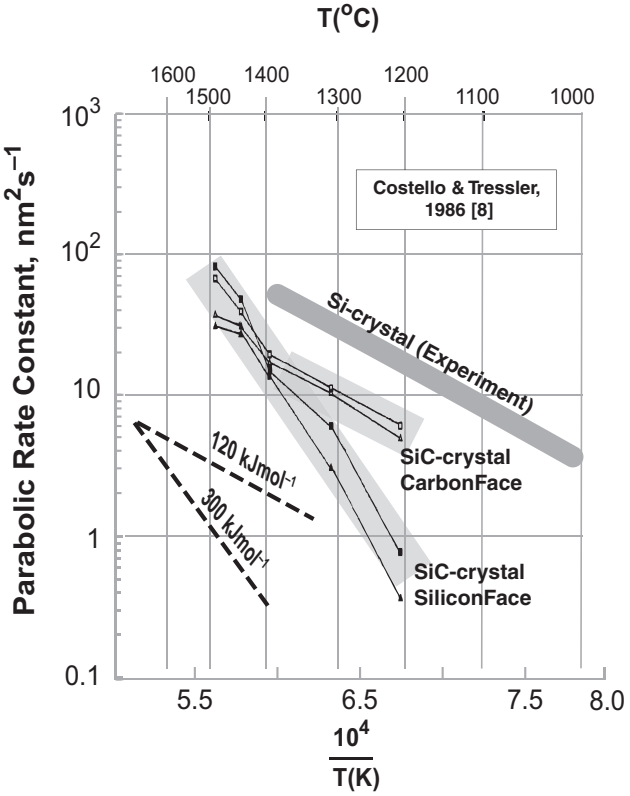

Fig. 3. A comparison of single crystal data from Costello and Tressler in comparison to Si.[1,8]

for the time-dependent or for the steady state. In this case, we assume the steady-state condition that the flux of oxygen molecules is uniform through the entire thickness of the oxide scale. This latter condition implicitly means that the divergence of oxygen flux is zero within the scale, that is, the oxygen molecules are neither created nor absorbed within the scale: this can occur only at the boundaries where the chemical potentials have been prescribed.

In the first instance, we assume that there is no interfacial barrier either to the insertion of oxygen into the overgrowth from the atmosphere, or to the reaction of oxygen with silicon at the buried interface. The gradient of the chemical potential through the scale is then given by the following equation:

$$\frac{d\mu_{O_2}}{dz} = -\frac{\mu^h_{O_2} - \mu^i_{O_2}}{h} \tag{2}$$

where $\mu^h_{O_2}$ is the potential at the surface and $\mu^i_{O_2}$ at the substrate–silica interface (the minus sign recognizes that diffusion occurs in the downhill direction of the potential gradient). At the surface, the potential is defined by the partial pressure of oxygen in the atmosphere, $p^h_{O_2}$, that is $\mu^h_{O_2} = RT \ln (p^h_{O_2})$For the oxidation of pure silicon, $\mu^i_{O_2}$ is exactly defined by the following reaction:

$$Si + O_2 = SiO_2 \tag{3}$$

which is held in equilibrium at the interface. The law of mass action gives the following equation:

$$RT \ln \frac{a^i_{SiO_2}}{a^i_{Si} a^i_{O_2}} + \Delta G_{SiO_2} = 0 \tag{4}$$

where the superscript i refers to the interface, and a to the activity of the species. ΔG_{SiO_2} is the free energy for the

reaction in Eq. (3).[11] In the oxidation of silicon, both silicon and silica exist in their pure state so that $a^i_{Si} = a^i_{SiO} = 1$. With this substitution, $a^i_{O_2}$, is obtained from Eq. (4). The potential gradient in Eq. (2) may now be written as follows:

$$\frac{d\mu_{O_2}}{dz} = -\frac{RT}{h}\ln\frac{p^h_{O_2}}{a^i_{O_2}} \tag{5}$$

Substituting Eq. (5) in Eq. (1), and recognizing that

$$\frac{dh}{dt} = J_{O_2} V_{SiO_2} \tag{6}$$

and further integrating from time, $t = 0$ to t gives the final result that

$$h^2 = k_p t \tag{7}$$

where k_p, the parabolic rate constant, is given by the following equation:

$$k_p = 2D_{O_2} n_{O_2} \ln\frac{p^h_{O_2}}{a^i_{O_2}} \tag{8}$$

Please be reminded that Eq. (8) assumes that there is no interfacial barrier to the ingress of oxygen into the glass from the atmosphere, and then again from the glass to its reaction to produce silica at the interface.

(2) Comparison with Experiment: Oxidation of Silicon

The result in Eq. (8) may be used to compare theory with experiment. The measurements for k_p for the oxidation of silicon single crystal in dry oxygen at 1 atm ($p^h_{O_2} = 1$) by D&G up to 1200°C and further up to 1400°C by Costello and Tressler[8] are reproduced in Fig. 4. We now proceed to compare these values with the prediction from Eq. (8).

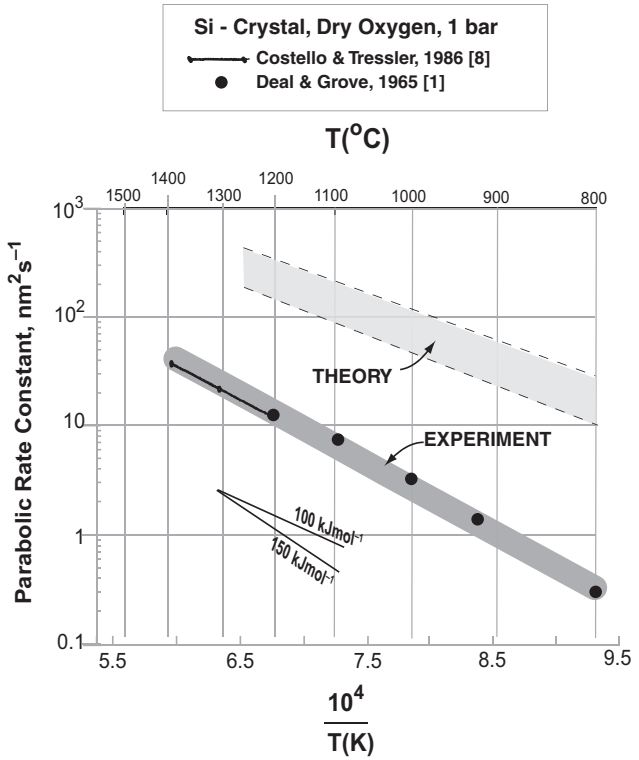

Fig. 4. Comparison of theory and experiment for oxidation of silicon crystals.

The diffusion coefficient in Eq. (1) refers to the transport of O_2 molecules in silica (as the parabolic rate constant has been unambiguously shown to be proportional to the oxygen pressure [1]). The other possibilities are diffusion of atomic oxygen, or diffusion of oxygen ions. However, these would require that the parabolic rate constant is proportional to the square root of the atmospheric pressure. Diffusion of oxygen ions would, in addition, require that a compensating charge of electron or holes be transported faster than the ions to maintain charge neutrality; the negligible electronic conductivity of silica makes such a scenario to be untenable.

Furthermore, oxygen atom and oxygen ion transport mechanisms are incompatible with the measured value for the activation energy for the parabolic rate constant; this value lies in the 1.2–1.3 eV range which is far less that would be required if oxygen atoms or ions were controlling oxygen transport. These points are discussed in greater detail in Appendix A.

Diffusion of O_2 has been determined by two methods: measurements of permeability through a glass "membrane", and by the use of isotopic $^{18}O_2$. The permeability measurements are straightforward as the flux is proportional to the product of the oxygen molecule diffusivity and the concentration of the species in the glass. The first quantity is obtained from the steady-state flux, and the second from the relaxation time to reach the steady state. Measurements by Norton and Hetherington and Jack belong to this method. The derivation of the permeability equation from Eq. (1) involves an assumption of a constant activity coefficient. This derivation is given in Appendix B.

The use of the $^{18}O_2$ to measure diffusivities requires care as interstitial molecules can exchange with the oxygen atoms in the –O–Si–O– network of the glass (imagine placing silica in pure isotopic gas—gradually all oxygen atoms in the network will be exchanged with ^{18}O). Therefore, isotope measurements involve several species: $^{18}O_2$, $^{18}\underline{O}$, O_2, and $\underline{O}$ where the underscore refers to the network species. As shown in Appendix A, the effective value for $(n_{O_2} D_{O_2})$ in the case where diffusion occurs additively by both interstitial O_2 and by network $\underline{O}$ is given by $(D_{O_2} n_{O_2} + \frac{1}{4} D_{\underline{O}})$. Also explained in Appendix B is why the network species are immobile relative to the interstitial molecules, so that the effective diffusion coefficient is still given by $D_{O_2} n_{O_2}$, as in Eq. (1). The use of isotope profiles to obtain diffusion measurements requires great care as the $^{18}O_2$ can exchange with $^{18}\underline{O}$, even if the network oxygens are relatively immobile. Therefore, isotope profiles will depend on time and temperature, eventually producing a uniform concentration of the isotope when the interstitial and network oxygens have exchanged to the fullest extent. At intermediate times, the isotope profiles can be difficult to deconvolute into the contributions from interstitial isotopes that diffuse, and the network oxygen isotopes that remain essentially frozen. When the soaking times in the isotope are short then the profiles are likely to reflect interstitial diffusion, but at long times they will merely give the concentrations of the isotope that have been incorporated into the network. This ambiguity has lead to a wide uncertainty in the diffusivities extracted from isotope profiles, as summarized in.[5,6,12] Again, these points are discussed further in Appendix A.

Here we use measurements by Norton[13] and Kajihara *et al.*,[14] which are summarized in Fig. 5. The data fall within a reasonably narrow band bounded by a factor of less than two. Both Norton and Kajihara *et al.* have measured the diffusion coefficient of molecular oxygen as well as the solubility of molecular oxygen in silica. Norton's measurements are direct having been made from the diffusion of oxygen by using glass as a permeable membrane. Kajihara *et al.* have employed an isotope optical fluorescence method, but were careful to measure at short times when the exchange with network oxygen had been negligible. Both sets of measurements

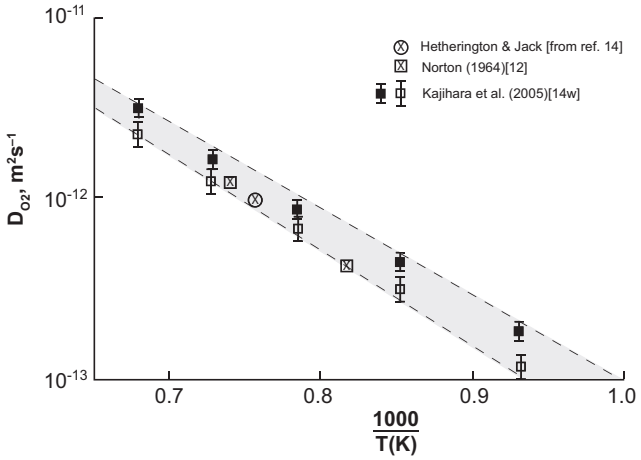

Fig. 5. Measurements of the diffusion coefficients for oxygen molecules in silica.

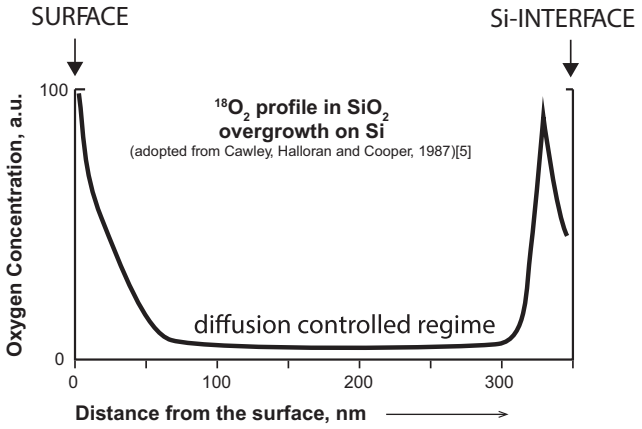

Fig. 6. Profile of oxygen in silica overgrowth. Adopted from Fig. 5 in Ref. [5] The isotope profile data were obtained in "double oxidation" measurements. An oxidation scale grown on silicon for 2 h at 960°C, was then exposed to ^{18}O for 3.5 min before obtaining the profile given above.

are consistent imparting credibility to the data summarized in Fig. 5.

The value of n_{O_2}, at one atmosphere oxygen pressure, has been obtained by Norton[13] and Kajihara.[14] They fall in the range of 2×10^{16}–3×10^{16} oxygen molecules per cm^3 of silica at one atmospheric pressure of dry oxygen and at 1000°C. Multiplying by the molar volume of silica (27.27 cm^3/mol) and dividing by the Avogadro's number gives that $n_{O_2} = 9.0 \times 10^{-7}$ to 1.4×10^{-6}. The dissolution of oxygen into silica is slightly exothermic (with an enthalpy of about 0.11 eV), but has been found to be essentially temperature independent above 1000°C (see fig. 5 in Ref. [14]).

It now remains to calculate the value for $a^i_{O_2}$, which is accomplished via Eq. (4), and is given by the following equation:

$$\ln(a^i_{O_2}) = \frac{\Delta G_{SiO_2}}{RT},$$

where,[11]

$$\Delta G_{SiO_2} = -901 + 0.175 \times T \text{ kJ/mol} \quad (9)$$

Substituting from Eq. (9) into Eq. (8), setting $p^h_{O_2} = 1$ (as the experiments were carried out in dry oxygen at one atmospheric pressure), and substituting for D_{O_2} from Fig. 5 and n_{O_2} as given in the preceding paragraph leads to the theoretical estimate of k_p which is compared with experiment in Fig. 4.

The experimental values for k_p are approximately one to two orders of magnitude slower than the theoretical prediction. This difference is attributed to n_{O_2} being lower under steady-state flux conditions (during oxidation), than in the conditions for the diffusion measurements reported in Refs. [13,14].

The argument for the lower concentration of interstitial oxygen is based upon the data from Ref. [5] which is adapted in Fig. 6. These data show the ^{18}O profile in the oxide overgrowth on silicon after being exposed to $^{18}O_2$ for 3.5 min at 960°C. This time is most likely too short for interstitial oxygen to have exchanged significantly with network oxygen, and is consistent with the experiments reported by Kajihara *et al.*[14] (At long times, the concentration becomes uniform as the interstitial oxygen exchanges completely with the network oxygen[5]). At the interfaces, the concentration changes sharply, but is essentially constant in the mid region of the oxide scale. In the steady state, the concentration and chemical potential gradients within the scale are determined by the boundary conditions for the chemical potential of oxygen at the surface and at the substrate interface. Within the scale they are defined by the condition that the flux of oxygen must be uniform. The concentration profile in Fig. 5 suggests that the flux through the scale is controlled by interface reactions, and is diffusion controlled in the large midsection of the scale. This finding is consistent with studies where interface control was measured in very thin overgrowths.[2,3] (The assumption that $^{18}O_2$ would have reached the steady state quickly in thin layers is not unreasonable as the solubility of O_2 is only 10^{-6}. Thus a small number of O_2 will saturate the silica. Nevertheless, it is well to keep in mind that this is still an assumption.)

The oxygen concentration in silica cannot exceed the equilibrium value. The maximum concentration in Fig. 6 can be assumed to be the equilibrium value. Therefore, in the diffusion-controlled regime, the oxygen concentration is very significantly lower. With this factor, the theory and experiment in Fig. 4 converge into reasonable agreement.

The above argument for the difference between experiment and prediction is based upon kinetics as O_2 concentration in the silica overlayer controls the flux, as given by Eq. (1). It is, however, also possible that the thermodynamic force for oxidation is reduced by the interface reaction, as illustrated in Fig. 7. As seen on the right-hand figure, the driving force for diffusion is the total difference in the chemical potential

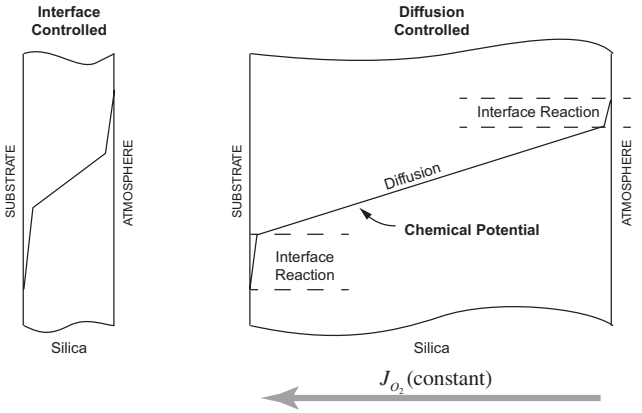

Fig. 7. The difference in the chemical potential between the atmosphere and the substrate, which is the total driving force for oxidation, is divided between interface reaction, which is independent of thickness and diffusion, which becomes shallower as the overgrowth thickens, leading to diffusion controlled oxidation behavior.

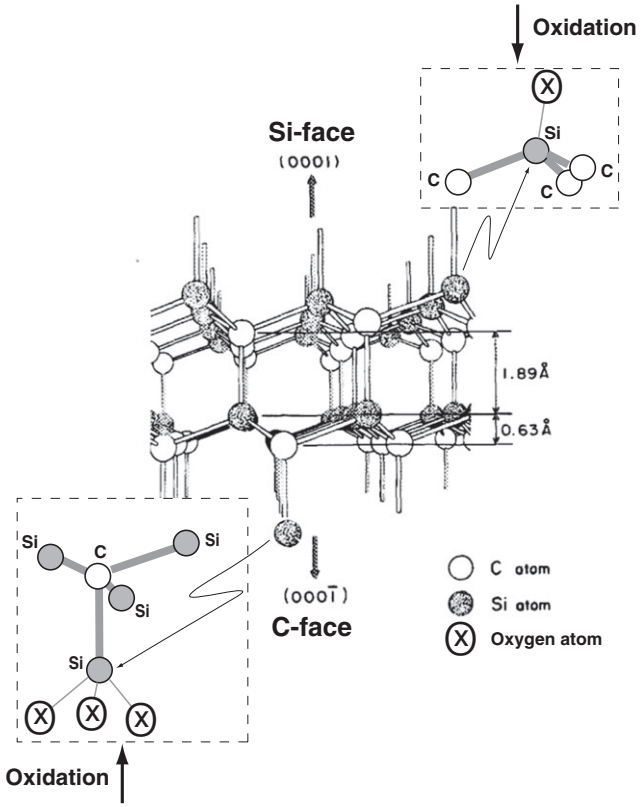

Fig. 8. The chemistry and coordination of the first monolayer on the C- and Si-faces of SiC. Note the higher Si:C ratio of atoms at the C-face.

between the atmospheric and the substrate interface minus the interfacial drop.

III. Oxidation of SiC Crystals

Similar to silicon, the oxidation of SiC also creates a passivating oxide scale of silica. However, there is a significant difference between the oxidation of SiC and of Si. In the case of Si, the chemical potential of oxygen at the interface is known since the activity of Si and SiO_2 are both unity. However, for silicon carbide the oxidation reaction is as follows:

$$SiC + \frac{3}{2}O_2 = SiO_2 + CO \tag{10}$$

The oxygen potential at the interface is still given by Eq. (4), however, a_{Si} is now determined by the equilibrium between silicon and carbon:

$$Si + C = SiC + \Delta G_{SiC} \tag{11}$$

so that

$$RT \ln \frac{a_{SiC}}{a_{Si} a_C} + \Delta G_{SiC} = 0 \tag{12}$$

where $a_{SiC} = 1$. The values a_{Si} and a_C can vary relative to one another, although their product remains constant. These values can change with the orientation of the crystal. Also noteworthy is that the activity of Si in SiC will be necessarily less than unity as the free energy of formation of SiC is negative. The oxygen potential at the interface will therefore vary with the activity of silicon, as in Eq. (4).It is with the above perspective that we consider the data for the oxidation of two different orientations of SiC given in Fig. 3, at temperatures up to 1500°C (near and above 1600°C the data in the literature do not consistently show parabolic behavior,[15] possibly because of the increasing significance of the volatilization of oxidation species). The orientations are sketched in Fig. 7, drawing upon Ref. [16]. The "carbon-face" gives a higher value for the parabolic rate constant than the "silicon-face". Moreover, whereas the activation energy for k_p^C is comparable to the oxidation of silicon, k_p^{Si} possesses a significantly higher activation energy.

(1) Orientation-Dependent Activity of Si

The difference between the C- and Si-faces of SiC lies in the chemistry and coordination of the first monolayer. In the C-face, each carbon atom on the surface is attached to three silicon atoms underneath. In the Si-face, the silicon atom is attached to three carbon atoms. Thus, the ratio of Si:C atoms is 3:1 at the C-face and 1:3 at the Si-face. It follows that the activity of Si is higher for the C-face and lower for the Si-face. In both instances, however, the activity of silicon is less than one.

Rewriting Eq. (4) after setting $a^i_{SiO_2} = 1$, we have that

$$p^i_{O_2} = \frac{1}{a^i_{Si_2}} e^{\frac{\Delta G_{SiO}}{RT}} \tag{13}$$

For a silicon crystal, $a^i_{Si_2} = 1$. In the case of SiC, as discussed just above, the activities of silicon will be lower and will have the following trend:

$$a^i_{Si}(\text{Si-face}) < a^i_{Si}(\text{C-face}) < a^i_{Si}(\text{Silicon}) \tag{14}$$

and, therefore, from Eq. (13),

$$p^i_{O_2}(\text{Si-face}) > p^i_{O_2}(\text{C-face}) > p^i_{O_2}(\text{Silicon}) \tag{15}$$

From Eq. (8), it then follows that

$$k_p(\text{Si-face}) < k_p(\text{C-face}) < k_p(\text{Silicon}) \tag{16}$$

The argument given above can therefore explain why the oxidation rate of the Si-face of SiC crystal is slower than the C-face and why both are slower than the oxidation rate of silicon crystal.

(2) Activity of Carbon

The result in Eq. (16) remains qualitative because the activity of Si cannot be calculated without the knowledge of the activity of C at the interface, as only their product is accessible from the thermodynamic data.

The activity of carbon is determined by the equilibrium of the following reaction at the interface:

$$C + \frac{1}{2}O_2 = CO \tag{17}$$

The activity of C therefore is determined by the p^i_{CO}, which is kinetically established by the diffusion of CO through the overgrowth out to the atmosphere.

(3) The Effective Diffusion Coefficient

The oxidation rate of SiC is determined by the rate at which oxygen can diffuse toward the substrate, the rate at which CO can diffuse out to the atmosphere, and the activity of Si at the interface. This coupled problem was analyzed in Ref. [17] for the oxidation of silicon oxycarbide, SiC_xO_y. It

reduces to oxidation of SiC by setting $x = 1,\ y = 0$, leading to the following expression for the effective diffusion coefficient[†] :

$$D_{\text{eff}} = 2\frac{2D_{O_2}n_{O_2}\cdot\frac{3}{2}D_{CO}n_{CO}}{2D_{O_2}n_{O_2}+\frac{3}{2}D_{CO}n_{CO}} \tag{18}$$

where D_{CO} is the coefficient of chemical diffusion, and n_{CO} is the solubility of CO in silica. The slower species controls D_{eff}, for example, if $D_{CO}n_{CO} << D_{O_2}n_{O_2}$, then $D_{\text{eff}} \approx 3D_{CO}n_{CO}$.

(4) Orientation-Dependent Oxidation of SiC Crystals

As seen in Fig. 3, the oxidation kinetics of SiC single crystals is slower than for silicon. Moreover, the Si-face oxidizes at a slower rate, and with a higher activation energy than the C-face. The activation energy for the C-face is similar to that for the oxidation of Si crystals.

The lower oxidation rate of SiC than Si can be explained by the lower activity of Si at the interface, as summarized in Eq. (16). A lower activity of silicon increases the oxygen potential as given by Eq. (15). The higher oxygen potential reduces the driving force for the diffusion of oxygen through the silica overgrowth. The relationship between k_p and $p^i_{O_2}$ is given by Eq. (8). In this way, it is reasonably well explained why the oxidation kinetics of the Si-face is lower than of the C-face and why both are lower than the rate of oxidation of Si crystal.

The activation energy for the oxidation of the C-face of SiC is in good agreement with the activation energy for Si, implying that in this instance the diffusion of oxygen through the silica overgrowth is rate controlling.

The higher activation energy for the Si-face is more difficult to explain. First, we must note that if two mechanisms, one having an activation energy that is higher than the other, act in series, that is, such that the slower of the two is rate controlling, then the one with the higher activation energy is likely to be dominant at low temperatures, and the lower activation mechanism at higher temperatures. The data in Fig. 3 show that below 1400°C the C-face oxidizes with a low activation energy, whereas the Si-face carries a higher activation energy.

In this problem, the two mechanisms of interest are (i) the inward diffusion of oxygen, and (ii) the outward diffusion of CO. Whichever is slower will be rate controlling. From the discussion just above, and with the recognition that below 1400°C the C-face activation energy agrees with the activation energy for the oxidation of Si (which is controlled by O_2 diffusion), we can argue that the oxidation of the Si-face is controlled by the outward diffusion of CO.

It is not possible to give a satisfying answer to the question why CO diffusion should become rate controlling for the Si-face. The effective diffusion coefficient, as given by Eq. (18) would apply equally to both orientations of the SiC crystal, unless the concentration of O_2 or of CO changes with orientation, which is a difficult argument to support in a concrete way. One hypothesis can be that the interface reaction at the Si-face lowers the concentration of CO in the bulk of the scale, which renders the rate-controlling mechanism in Eq. (18) to change from O_2 diffusion to CO diffusion.

IV. Discussion

The oxidation kinetics of Si-based substrates is almost always analyzed by assuming that the flux of oxygen is proportional to the concentration gradient as prescribed by the Fick's law. However, the data given in Fig. 6, which has been confirmed by other investigators, does not support this approach: the concentration gradients are not evident and the high concentrations near the interface would require uphill diffusion.

Here, we consider the kinetics in terms of chemical potentials and chemical diffusion coefficients, which is the usual way for analyzing the rates of chemical reactions. For example, the chemical potential approach can explain spinodal decomposition where B diffuses uphill toward precipitates rich in B within a solid solution of B in A.

In terms of chemical potentials, the "boundary value" problem for silica overgrowth (in quasi steady state) is constrained by two conditions: (i) the values of the chemical potential of O_2 at the silica–atmosphere and the silica–substrate interfaces are fully prescribed, and (ii) a J_{O_2}, the flux through the thickness of silica overgrowth must remain constant through the entire thickness. There are two unknowns in the problem: determination of whether the transport is diffusion controlled or interface controlled, and the atomistic mechanism of O_2 transport. As has been discussed in this article, the parabolic behavior confirms diffusion control, and the activation energy points toward interstitial diffusion of O_2. It is reasonable to assume that the chemical potential assumes a profile as shown in Fig. 7, where there are drops at the two interfaces to account for interface reaction and a uniform gradient through the thickness for diffusion according to Eq. (1), with the latter being rate controlling. Note that a constant value of the flux for a constant gradient of the potential requires that the concentration through the thickness remains constant, which is consistent with the data shown in Fig. 6.

It is well to keep in mind that the an equilibrium between the chemical potential and the concentration within the overgrowth can be enforced only if the material within the overgrowth can equilibrate with a gas at the corresponding partial pressure of oxygen, which is clearly not possible. Therefore, the concentration profile within the overgrowth is constrained not by equilibrium, but by the condition of a constant value of J_{O_2}, that is given as follows:

$$J^{(1)}_{O_2} = J^{\text{diff}}_{O_2} = J^{(2)}_{O_2} \tag{19}$$

where $J^{(1)}_{O_2} = \delta_1 k_1 \Delta c^{(1)}_{O_2}$ is the interface reaction flux, k_1 is the jump frequency across the interface, δ_1 is the jump distance that is the effective width of the interface, and $\Delta c^{(1)}_{O_2}$ is the concentration difference across the interface. Here, superscripts (1) and (2) refer to the atmosphere–silica and the silica–substrate interfaces, respectively. The middle term, $J^{diff}_{O_2}$ is the same as Eq. (1). The concentration profiles must adjust to meet the condition given by Eq. (19).

As discussed under Introduction, the interface reaction can be rate controlling in the early stage of oxidation, but not for thick overgrowths when diffusion control becomes rate limiting. The analysis in this article centers on this diffusion-controlled regime.

V. Summary

1. Oxygen diffuses as O_2 molecules through the silica overgrowths.[1] The theoretical estimate of the activation energy based upon the molecules diffusing without breaking the bonds in the glass network[7] is in agreement with the experiment. It follows that oxygen permeation depends upon the product of tracer diffusion coefficient and the solubility of O_2 in the glass.
2. The influence of solubility is accounted for by formulating oxygen transport in terms of the chemical potentials of oxygen. In this boundary value problem, the flux remains constant through the silica overgrowth, with O_2 being inserted and absorbed at the surface

[†]In Ref. [17] the factor n_{O_2} was erroneously omitted because it was assumed that oxygen diffuses as a part of the silica network. Instead, oxygen diffuses as an "independent" molecular species.

and at the substrate interface where the chemical potentials of oxygen are defined.
3. The theoretical estimate of the parabolic rate constant by the above approach overestimates k_p by a factor of 10–100.
4. This discrepancy is explained by the high concentration gradient of O_2 at the interfaces,[5] which lowers the oxygen concentration in the broad diffusion regime through the thickness of the silica scale. With this correction, a reasonable agreement between theory and experiment is possible.
5. The lower rates of oxidation of SiC single crystals can be explained by the lower activity of Si (than in Si crystal) at the interface. The interface structure of the C-face and the Si-face of SiC single crystals can explain why the oxidation rate is slower for the Si-face.
6. The activation energy for the oxidation of the Si-face is greater than, and diverges increasingly from the lower activation energy for the C-face at lower temperatures, suggesting two possible rate-controlling mechanisms with the slower one being important for the oxidation of the Si-face. It is hypothesized that the higher activation energy for the Si-face arises from diffusion (and solubility) of CO through the silica overgrowth.

Appendix A

^{18}O Measurements and Interactions Between Interstitial O_2 and Network $\underline{O}$

Diffusion Mechanism(s): Theoretically, oxygen can be transported through silica as three different species: (i) molecules of O_2 that diffuse through the interstitial spaces without exchanging bonds with the silica network, (ii) as oxygen atoms, O, that are members of the silica network and migrate by breaking and making the Si–O bonds in the network, and (iii) as oxygen ions, O^{2-}, that also migrate interstitially as an independent species.

All three mechanisms of oxygen transport listed above are additive, that is, they can be summed to obtain the total oxygen flux through the silica scale.

The transport by O^{2-} may be set aside as it would require the transport of electrons or Si^{4+} as well to maintain charge neutrality. There is little evidence so far to support that the electronic conductivity or the diffusivity of Si^{4+} is likely to be as fast as the diffusion of O^{2-}.

The transport of O_2 may now be written as the sum of the diffusion of interstitial O_2 and the network $\underline{O}$. Extending Eq. (1) to include the diffusion of both species we have that

$$J_{O_2} = -\left(\frac{D_{O_2} n_{O_2}}{V_{SiO_2} RT}\frac{d\mu_{O_2}}{dz} + \frac{1}{2}\frac{D_{\underline{O}}}{V_{SiO_2} RT}\frac{d\mu_{\underline{O}}}{dz}\right) \tag{A1.1}$$

Note that $n_{\underline{O}} = 1$ as its molar concentration is unity (assuming that the network oxygen vacancies are scarce). The factor of 0.5 in the second term arises because two $\underline{O}$ must be transported to achieve the diffusion of one oxygen molecule. The question then arises as to which of the two terms is more important for the transport of oxygen.

The fundamental driving force for the diffusion of oxygen is the difference in the activity of oxygen in the atmosphere and at the substrate–silica interface. The activity of oxygen in the atmosphere can be equated to the atmospheric pressure of oxygen where 1 atm is the standard state. Thus, the atmospheric pressure sets the boundary condition for μ_{O_2} at the silica–gas interface. The activity of oxygen at the substrate interface is determined by the oxidation reaction between it and oxygen (in the case of silicon carbide, the relative outward diffusivity of oxygen and carbon monoxide would determine their relative activities).

When the oxidation is taking place in a quasi steady state, when interstitial oxygen has reached equilibrium with the network oxygen, the following thermodynamic constraint applies:

$$\mu_{O_2} = 2\mu_{\underline{O}} \tag{A1.2}$$

which, when substituted in (A1.1) gives the following equation:

$$J_{O_2} = -\frac{1}{4V_{SiO_2} RT}\frac{d\mu_{O_2}}{dz}\left(4D_{O_2} n_{O_2} + D_{\underline{O}}\right) \tag{A1.3}$$

The activation energy for the oxidation rate, which is proportional to J_{O_2}, depends on the activation energies for $D_{O_2}(Q_{O_2})$, for $D_{\underline{O}}(Q_{\underline{O}})$, the heat of solution of oxygen molecules into the silica lattice, which, from experiments,[14] has been found to be negligible in the temperature range of interest. Studies from oxidation of silicon[1] and of the diffusion of molecular oxygen through silica[13] have consistently shown that $Q_{O_2} = 110 - 130$ kJ/mol. Theoretical estimates for $Q_{\underline{O}}$, which would be approximately equal to the strength of two Si–O bonds (in a silica network), predict it to be 400 kJ/mol[7] or higher. Experiments with CVD silicon carbide up to ~1550°C[18] show that that the activation energy remains unchanged at ~120 kJ/mol, leading to a reasonable inference that D_{O_2} is rate controlling in the oxidation of SiC.

(The dominance of the first diffusion term in Eq. (A1.3) depends not only on the activation energy but also on n_{O_2} which has been measured to be $\sim 10^{-6}$.[13,14] However, even with this "weighting factor", the first term dominates in the 1300°C–1550°C range if the difference between the two activation energies is 300 kJ/mol or greater.)

^{18}O Isotope Profiles

The activation energy measurements show that oxygen diffuses through the silica overgrowths by interstitial molecules, with the network oxygen atoms remaining relatively "frozen". However, the interstitial oxygen can continue to exchange with network oxygen as time progresses, even if this process is slower than the diffusion of molecular interstitial oxygen.

The measurement of oxygen isotope profiles, therefore, will depend not on the diffusion of interstitial oxygen, but instead on the rate at which oxygen is incorporated into the network. After a long period of exposure, especially at high temperatures, to $^{18}O_2$ the network will become essentially saturated with ^{18}O, and its concentration will become uniform across the scale thickness: this is indeed what has been observed.[5] At shorter times, the ^{18}O profile is likely to be determined in a complex way by both the diffusion of O_2 and the exchange between interstitial oxygen molecules and $\underline{O}$. The interpretation of these results is, therefore, ambiguous, with several free variables such as the exchange rate between O_2 and $\underline{O}$, and the diffusion of interstitial O_2. During this transient period, all that can be said is there would be a correlation between the special concentrations of O_2 and $\underline{O}$, as the exchange rate will be proportional to these concentrations. However, careful measurements taken over times that are short enough to preempt any significant exchange with network oxygen can lead to credible measurements of the diffusion coefficient.[14]

Appendix B

Relating Eq. (1) to Measurements of Permeability

Measurements of the steady-state flux of oxygen molecules through a thin silica "membrane" driven by a pressure difference on two sides was used by Norton to measure the

diffusivity of oxygen molecules. The flux varied linearly with pressure confirming that oxygen was transporting as molecular species. The basic equation for this measurement can be written in the following form:

$$J_{O_2} = -c^*_{O_2} D_{O_2} \frac{dp_{O_2}}{dz} \tag{A2.1}$$

where J_{O_2} is the steady-state flux of O_2 in $\#m^{-2}s^{-1}$, $c^*_{O_2}$ is the concentration of O_2 molecules per unit volume per unit pressure (e.g., $\#m^{-3}atm^{-1}$, where pressure is measured in units of atmospheres), D_{O_2} is the diffusivity in units of m^2/s, and (dp_{O_2}/dz) is the pressure gradient in units of atm/m. The minus sign insures that molecular flow occurs in the downhill direction of the pressure gradient. The objective of this exercise was to determine the conditions under which Eq. (1) reduces to Eq. (A2.1).

We begin by writing Eq. (1) in the following form:

$$J_{O_2} = -\frac{D_{O_2} c_{O_2}}{k_B T} \frac{d\mu_{O_2}}{dz} \tag{A2.2}$$

here, c_{O_2} is the concentration in units of $\#m^{-3}$, and R has been replaced by k_B to convert moles into #molecules. Recall that μ_{O_2} is the chemical potential of the species O_2 in the glass. Writing it as a function of the *molar* concentration of O_2, written as x_{O_2}, and the activity coefficient, γ_{O_2}:

$$\mu_{O_2} = \mu^o_{O_2} + k_B T \ln(\gamma_{O_2} x_{O_2}) \tag{A2.3}$$

where $\mu^o_{O_2}$ is the reference potential (e.g., one atmospheric pressure). Differentiating Eq. (A2.3) and substituting into Eq. (A2.2) gives the following result:

$$J_{O_2} = -D_{O_2}\left(1 + \frac{d\ln\gamma_{O_2}}{d\ln x_{O_2}}\right)\frac{dc_{O_2}}{dz} \tag{A2.4}$$

where the following substitution has been made:

$$\frac{dx_{O_2}}{x_{O_2}} = \frac{dc_{O_2}}{c_{O_2}} \tag{A2.5}$$

as Eq. (A2.5) is written in dimensionless (normalized) form.

It now remains to enforce the equilibrium between the O_2 molecules in the gas phase with those dissolved in the solid according to the following reaction:

$$O_2^g = O_2 + \Delta G_{O_2} \tag{A2.6}$$

where ΔG_{O_2} is the change in free energy when a molecule in the gas phase is inserted into the solid. By law of mass action we have that

$$\Delta G_{O_2} + k_B T \ln \frac{\gamma_{O_2} x_{O_2}}{p_{O_2}} = 0 \tag{A2.7}$$

where the activity of oxygen in the gas phase is, by convention for the standard state, equated to the pressure measured in atmospheres. Recognizing that $\Delta G_{O_2} = \Delta H_{O_2} - T\Delta S_{O_2}$, where ΔH_{O_2} is the heat of mixing and ΔS_{O_2} is the change in the vibrational entropy of the molecule in the gas and in the solid, we obtain that

$$\gamma_{O_2} x_{O_2} = p_{O_2} e^{\frac{\Delta S_{O_2}}{k_B}} e^{-\frac{\Delta H_{O_2}}{k_B T}} \tag{A2.8}$$

The temperature dependence of the solubility is then given by the term on the far right. Experiments have shown the solubility to be nearly temperature independent,[14] meaning that $\Delta H_{O_2} \simeq 0$, which leads to the following simplification:

$$x_{O_2} = \left(\frac{1}{\gamma_{O_2}} e^{\frac{\Delta S_{O_2}}{k_B}}\right) p_{O_2} \tag{A2.9}$$

Equation (A2.9) states that the solubility of O_2 molecules in the glass will be proportional to p_{O_2} only if the activity coefficient is independent of concentration. In this case, the terms within the brackets becomes a constant of proportionality. If the concentration is defined per unit pressure then it follows that

$$c_{O_2} = c^*_{O_2} p_{O_2} \tag{A2.10}$$

where $c^*_{O_2}$ is the solubility, that is, the number of molecules per unit volume per unit of atmospheric pressure.

If the activity coefficient is indeed independent of the concentration then the term within the brackets in Eq. (A2.4) reduces to unity. Substituting from Eq. (A2.10), we obtain the final result that

$$J_{O_2} = -D_{O_2} c^*_{O_2} \frac{dp_{O_2}}{dz} \tag{A2.11}$$

Norton's experiments measured the diffusion coefficient and the solubility of oxygen molecules in silica. It is important to remember that Eq. (A2.11) is valid only if the activity coefficient is independent of the concentration, which also implies that the solubility remains linearly proportional to the gas pressure.

Acknowledgments

This work was supported by the US AFOSR (Dr. Ali Sayir) and NASA (Dr. Anthony Calomino) under the National Hypersonic Science Center for Materials and Structures (AFOSR Contract No. FA9550-09-1-0477). Helpful discussions with my doctoral student, Kalvis Terauds, and colleague, David B. Marshall, are gratefully acknowledged. Special thanks to Dr. Krishan L. Luthra for asking probing questions and stimulating critical thinking.

References

[1]B. Deal and A. Grove, "General Relationship for Thermal Oxidation of Silicon," *J. Appl. Phys.*, **36** [12] 3770–8 (1965).

[2]P. Thanikasalam, T. Whidden, and D. Ferry, "Oxidation of Silicon (100): Experimental Data Versus a Unified Chemical Model," *J. Vac. Sci. Technol., B*, **14** [4] 2840–4 (1996).

[3]A. Bongiorno and A. Pasquarello, "Dependence of the O-2 Diffusion Rate on Oxide Thickness During Silicon Oxidation," *J. Phys.-Condens. Matter*, **15** [16] S1553–60 (2003).

[4]K. Luthra, "Some New Perspectives on Oxidation of Silicon-Carbide and Silicon-Nitride," *J. Am. Ceram. Soc.*, **74** [5] 1095–103 (1991).

[5]J. Cawley, J. Halloran, and A. Cooper, "O-18 Tracer Study of the Passive Thermal-Oxidation of Silicon," *Oxidation Metals*, **28** [1–2] 1–16 (1987).

[6]J. Kalen, R. Boyce, and J. Cawley, "Oxygen Tracer Diffusion in Vitreous Silica," *J. Am. Ceram. Soc.*, **74** [1] 203–9 (1991).

[7]A. Stoneham, M. Szymanski, and A. Shluger, "Atomic and Ionic Processes of Silicon Oxidation," *Phys. Rev. B*, **63** [24] 241304, 4pp (2001).

[8]J. Costello and R. Tressler, "Oxidation-Kinetics of Silicon-Carbide Crystals and Ceramics .1. in Dry Oxygen," *J. Am. Ceram. Soc.*, **69** [9] 674–81 (1986).

[9]Z. Zheng, R. Tressler, and K. Spear, "Oxidation of Single-Crystal Silicon-Carbide .1. Experimental Studies," *J. Electrochem. Soc.*, **137** [3] 854–8 (1990).

[10]V. Presser and K. G. Nickel, "Silica on Silicon Carbide," *Crit. Rev. Solid State Mater. Sci.*, **33** [1] 1–99 (2008).

[11]D. R. Gaskell, *Introduction to Metallurgical Thermodynamics*. 498pp, McGraw Hill, New York, 1973.

[12]R. Meek, "Diffusion-Coefficient for Oxygen in Vitreous SiO_2," *J. Am. Ceram. Soc.*, **56** [6] 341–2 (1973).

[13]F. Norton, "Permeation of Gaseous Oxygen Through Vitreous Silica," *Nature*, **191** [478] 701 (1961).

[14]K. Kajihara, H. Kamioka, M. Hirano, T. Miura, L. Skuja, and H. Hisono, "Interstitial Oxygen Molecules in Amorphous SiO_2. III. Measurements of Dissolution Kinetics, Diffusion Coefficient, and Solubility by Infrared Photoluminescence," *J. Appl. Phys.*, **98** [1] 013529, 7pp (2005).

[15]T. Narushima, T. Goto, Y. Yokoyama, M. Takeguchi, Y. Iguchi, and T. Hirai, "Active-To-Passive Transition and Bubble Formation for High-Temperature Oxidation of Chemically Vapor-Deposited Silicon-Carbide in Co-Co_2 Atmosphere," *J. Am. Ceram. Soc.*, **77** [4] 1079–82 (1994).

[16]L. Muehlhoff, W. J. Choyke, M. J. Bozack, and Y. T. Yates, "Comparative Electron Spectroscopic Studies of Surface Segregation on SiC(0001) and SiC(000-1)," *J. App. Phys.*, **60** [8] 2842–53 (1986).

[17]S. Modena, G. Soraru, Y. Blum, and R. Raj, "Passive Oxidation of an Effluent System: The Case of Polymer-Derived SiCO," *J. Am. Ceram. Soc.*, **88** [2] 339–45 (2005).

[18]C. E. Ramberg and W. L. Worrell, "Oxygen Transport in Silica at High Temperatures: Implications of Oxidation Kinetics," *J. Am. Ceram. Soc.*, **84** [11] 2606–17 (2001). □